

# Gravitational wave backgrounds from colliding exotic compact objects

Hannah Banks<sup>1,2</sup>, Dorota M. Grabowska<sup>3,2</sup> and Matthew McCullough<sup>2</sup>

<sup>1</sup>*DAMTP, University of Cambridge, Wilberforce Road, Cambridge, CB3 0WA, United Kingdom*

<sup>2</sup>*Theoretical Physics Department, CERN, 1211 Geneva 23, Switzerland*

<sup>3</sup>*InQubator for Quantum Simulation (IQUS), Department of Physics, University of Washington, Seattle, Washington 98195, USA*



(Received 12 May 2023; accepted 20 July 2023; published 14 August 2023)

Long-baseline atom interferometers offer an exciting opportunity to explore midband gravitational waves with frequencies of 1 mHz–10 Hz. In this work we survey the landscape of possible contributions to the total gravitational wave background from merging binary systems in this frequency band and advocate for targeting this observable. Such an approach is complimentary to searches for resolved mergers from individual sources and may have much to reveal about the Universe. We highlight that the inspiral phases of known stellar-mass compact binaries cumulatively produce a signal well within reach of the proposed AION-km and AEDGE experiments which will need to be accounted for in the gravitational wave programs of these experiments. We further show that hypothetical populations of dark sector exotic compact objects, harboring just a tiny fraction of the dark energy density, could generate signatures unique to gravitational wave detectors sensitive to subhertz frequencies, providing a novel means to probe complexity in the dark sector.

DOI: [10.1103/PhysRevD.108.035017](https://doi.org/10.1103/PhysRevD.108.035017)

## I. INTRODUCTION

The pursuit for fundamental physics beyond the Standard Model (SM) is entering a new era. It is becoming increasingly attractive to explore the possibility that the solutions we seek have remained hidden not behind a currently unattainable energy barrier, but through incredibly weak couplings to the SM. Recent developments in quantum sensing technologies have unlocked a host of new avenues through which to probe this “feebly interacting frontier” (see, e.g., Refs. [1,2]). By measuring the phase difference between atomic matter waves traveling along different paths, atom interferometry is one such class of experiment that offers exciting opportunities to probe physics at the quantum level [3–10]. By coupling state-of-the-art developments in the technologies deployed in atomic clocks with established methods of constructing inertial sensors, it has become feasible to consider upscaling conventional tabletop experiments in order to reach lower operational frequencies. Five long-baseline terrestrial prototype atom interferometry experiments, AION-10 [11] in the UK, MAGIS-100 [12] in the U.S., MIGA [13] in France, VLBAI [14] in Germany, and ZAIGA [15] in

China, have currently been commissioned and are under construction, serving as essential technology readiness indicators to the deployment of kilometer-scale terrestrial detectors by the mid-2030s. In addition to providing opportunities to search for exotic forces [14,16–21] and hidden sectors of particles [22,23], experiments like AION-km, MAGIA-advanced, ELGAR [24], MAGIS-km, and advanced-ZAIGA, will open a unique window to the midfrequency  $\sim$ millihertz–10 Hz gravitational wave (GW) landscape [25–32], bridging the gap in frequencies that will exist between the LIGO [33,34] and LISA [35] detectors. Proposals for space-based cold-atom interferometers, most notably AEDGE [36], are also under serious consideration and would allow for an even more complete exploration of this uncharted phenomenological territory. For the purpose of example, this work will be primarily concerned with the AION-km experiment, and its possible successor AEDGE. Although to be realized using different cold-atom technologies, with predicted sensitivities to GWs of a similar order of magnitude, we expect the conclusions reached in this work to also be of relevance to other future kilometer-scale atom interferometry experiments.

To date, the science cases for the GW programs of kilometer-scale atom interferometers have largely, but not entirely, focused on the possibility of detecting resolved mergers of individual intermediate-mass black hole binary systems. There have also been proposals to search for stochastic signals arising from early Universe first-order

---

*Published by the American Physical Society under the terms of the Creative Commons Attribution 4.0 International license. Further distribution of this work must maintain attribution to the author(s) and the published article's title, journal citation, and DOI.*

phase transitions or cosmic strings [11,12,32]. The prospective sensitivities of AION-km and AEDGE to such signals are considered in Refs. [11,36] and explored more comprehensively in Ref. [37]. In this work we examine the AION capabilities through an alternative lens, turning instead to the cumulative signals or “gravitational wave backgrounds” (GWBs) that arise from the incoherent superposition of the radiation from large numbers of, for the most part, individually unresolvable merging binary systems [38]. While their peak emission occurs at the point of merger in the LIGO frequency band ( $\sim 10^2$ – $10^4$  Hz) [39], stellar-mass astrophysical compact binary systems produce a continuous spectrum of lower frequency gravitational radiation during their inspirals. Using the distributions and merger rates [40,41] of these populations as inferred from direct observations at the LIGO-Virgo network [42,43], we demonstrate that the cumulative background from these LIGO-Virgo populations of compact binaries is well within the experimental reach of both terrestrial- and space-based future long-baseline atom interferometers. As well as being a relevant and previously unaccounted for background to these experiments that needs to be mapped out to assess their sensitivity to other, perhaps more exotic, sources of GWs, measurements of this signal itself could have much to tell us.

Several calculations of the backgrounds from mergers of the LIGO-Virgo astrophysical populations have been presented previously in literature (see for example Refs. [44–49]), including Ref. [41] which is based on the most up-to-date LIGO-Virgo catalog GWTC-3 [43] including events from the second half of the third observational run (O3). Despite this, the implication of an astrophysical background to the midfrequency band (millihertz–10 Hz) GW searches proposed at terrestrial long-baseline atom interferometers has received very little attention, something which we hope to address with this work. We begin in Sec. II by establishing a general procedure for calculating the total gravitational background signal from a given population of merging compact objects. In Secs. II A, II B, and II C we then apply this framework specifically to the populations of stellar-mass binary black holes (BBHs), binary neutron stars (BNSs), and black hole–neutron star (BHNS) binary systems that have been inferred from observations at the LIGO-Virgo network in order to estimate their combined total signal in the AION frequency band. In addition to forming a relevant background to more exotic sources of GW, we argue that this signal offers an interesting science case from both an astrophysical and fundamental physics perspective, meriting close attention in its own right. Although we expect these populations to dominate the total astrophysical background for terrestrial-based long-baseline atom interferometers, in Sec. II D we comment on alternative sources that may be of relevance, particularly at the lower frequencies that are to be reached in future space-based experiments. With no empirical data to inform the estimation of their distributions and merger rates,

the uncertainty on the GWB from such alternative sources is considerably greater than that of their LIGO-Virgo observed counterparts and as such we do not include them in our estimation of the total astrophysical background.

Given the rich landscape of astrophysical structures present in the vastly subdominant visible sector of the Universe, it is reasonable to assume that the dark sector may harbor similar diversity. Indeed, the coalescence of dark particles or exotic states of Standard Model particles into a stable astrophysical-size exotic compact objects (ECOs) has been a subject of much recent attention in literature [50–52]. Examples of ECOs include fermion stars [53–60], boson stars [61–66], dark matter stars [67], and Proca stars [68]. These ECOs fit into a paradigm for dark matter where elementary particles form exotic composite objects with exponentially large occupation numbers. Since the mass of these objects span many decades, they must be searched for in a multitude of ways, including both terrestrial and nonterrestrial methods [69–78]. Returning to ECOs specifically, if these objects form binary systems, the gravitational radiation resulting from their mergers would contribute to the overall background, much in the same way as their SM counterparts, and could potentially be observable. Estimates of the background signals from a handful of specific types of binary ECOs, namely boson stars and dark blobs, are considered in Refs. [79,80], respectively. Here, we attempt to take a more general approach, keeping our analysis as model independent as we can and classifying signals only in terms of the mass scale of the binaries involved. In Sec. III we show that even if such populations only comprise a very small fraction of the dark matter budget, they could generate detectable signals in the frequency band to be probed by long-baseline atom interferometers. Combining measurements of the cumulative background at experiments operating in complimentary frequency ranges, this signal could be distinguishable from the dominant SM background, giving long-baseline atom interferometers a unique capability to probe the possible existence, formation history, and distribution of these structures, and as such, complexity in the dark sector.

## II. GW BACKGROUNDS FROM COMPACT BINARY MERGERS

We shall begin by clarifying exactly what we mean by a gravitational wave background. Although just a small fraction of the rich and diverse GW landscape, the only direct detections of gravitational radiation to date have been from isolated pointlike sources that generate coherent, resolvable signals [81]. In practice, however, many signals that reach any given GW detector cannot be resolved. This occurs when individual signals are too weak or when they are too closely spaced in time to be separated [82]. The total gravitational emission from a given population of sources, including both resolvable and unresolvable signals, is an intrinsic property of the

Universe [46] and forms what we shall refer to as the GWB for that source type. It is this, summed over all possible source types, that may be measured by the detector. If the resolvable signals are subsequently removed, the remaining “residual” background, composed from the incoherent accumulation of individually unresolved signals, can be analyzed stochastically. This stochastic gravitational wave background (SGWB) is thus detector dependent and can receive both astrophysical and cosmological (primordial) contributions [83]. The cosmological background is vastly subdominant [84], and much thought has been given to determine ways of distinguishing it from the astrophysical stochastic background; see for example Refs. [45,85–88]. A comprehensive, recent review of the SGWB and its various SM sources can be found in Ref. [82]. In reality, the practice of removing resolved signals is far from straightforward, as it is detector dependent and involves a number of subtleties [82]. Given this, and accounting for the fact that in this work we shall consider several different detectors of which the experimental details are not yet certain, we shall only concern ourselves with the total GWB and not attempt to exclude potentially resolvable sources from our computations.<sup>1</sup>

We shall henceforth review the formalism for computing the GWB from a generic, known population of compact binary systems. Throughout we shall adopt the convention that the speed of light  $c = 1$ , assume a flat standard  $\Lambda$  cold dark matter cosmology with  $\Omega_m = 0.3065$  and  $\Omega_\Lambda = 1 - \Omega_m$ , and take the Hubble constant  $H_0$  to be 67.9 km/s/Mpc, as measured by the Planck Collaboration [90].

GWBs can be conveniently characterized in terms of their energy density spectrum via the dimensionless quantity [38]

$$\Omega_{\text{GW}}(f) = \frac{f}{\rho_c} \frac{d\rho_{\text{GW}}(f)}{df}, \quad (1)$$

where  $d\rho_{\text{GW}}$  is the total energy density in the observed frequency range  $f$  to  $f + df$ , and  $\rho_c = 3H_0^2/(8\pi G)$  is the critical density needed to close the Universe.

If one specifies to the GWB from mergers of a population of binary compact objects with constituent masses  $m_1$  and  $m_2$  located at a redshift  $z$ , this can be further expressed as [48]

<sup>1</sup>We note that some works refer to any cumulative calculation of gravitational wave emission from a set of sources as a contribution to the SGWB even if resolved signals are not excluded. While this may be practical given the large uncertainties and degree of choice involved in any subtraction procedure, for the background to be stochastic in a statistical sense, any potentially resolvable astrophysical signal should be removed. This distinction of terminology is only relevant for the calculation of cumulative signals from populations of objects whose individual signals are not intrinsically stochastic, not where the sources are inherently stochastic, such as those of cosmological origin [82,89].

$$\Omega_{\text{GW}}(f) = \frac{f}{\rho_c H_0} \int_0^{z_{\text{max}}} dz \int dm_1 dm_2 \frac{d\mathcal{R}(z)}{dm_1 dm_2} \frac{d\tilde{E}_{\text{GW}}}{df_s} \times \frac{1}{(1+z)E(z)}. \quad (2)$$

Here,  $f_s$  refers to the emission frequency in the source frame, which is related to  $f$ , the frequency measured at the detector, by  $f_s = f(1+z)$ . Additionally,  $\frac{d\mathcal{R}(z)}{dm_1 dm_2}$  is the differential rate of mergers per comoving volume element and  $\frac{d\tilde{E}_{\text{GW}}}{df_s}$  is the source frame energy spectrum from a single binary system. The function  $E(z)$  is defined as  $\sqrt{\Omega_m(1+z)^3 + \Omega_\Lambda}$ .

This expression can be recast as [45]

$$\Omega_{\text{GW}} = \int dm_1 dm_2 \int \frac{dV_c}{1+z} \frac{d\mathcal{R}(z)}{dm_1 dm_2 \rho_c} \frac{1}{df} \frac{d\tilde{\rho}_{\text{GW}}(m_1, m_2)}{df}, \quad (3)$$

where  $\frac{d\tilde{\rho}_{\text{GW}}}{df}$  is the comoving energy density spectrum of a single binary system in the detector frame, and  $dV_c$  is the comoving volume element. The former is directly related to the amplitude of the Fourier transform of the detected signal  $|\tilde{h}(f)|$  according to [91]

$$d\tilde{\rho}_{\text{GW}} = \frac{4}{5} \frac{\pi}{G} f^3 |\tilde{h}(f)|^2 df, \quad (4)$$

where the factor of 4/5 accounts for averaging over possible source orientations [92,93].

Although  $|\tilde{h}(f)|$  is specific to the class of objects merging and is in general not analytically tractable, it is worth pointing out that the dominant contribution to the background comes from the inspiral phase of the merger. Here, the binary constituents are widely separated and the system can be well approximated by a pair of self-gravitating point masses emitting gravitational quadrupole radiation. This calculation is both analytic and irrespective of the specific nature of the objects involved and results in a contribution to  $\Omega_{\text{GW}}$  that scales as  $f^{2/3}$  [94].

The final component of the calculation is the differential merger rate  $\frac{d\mathcal{R}(z)}{dm_1 dm_2}$ , which encodes both the redshift and mass distributions of the population in question. Taking these distributions to be decoupled, this can be expressed as [45]

$$\frac{d\mathcal{R}(t)}{dm_1 dm_2} = \frac{R_0}{Z} P_m(m_1, m_2) \times \int dt_d dz_b P_b(z_b) P_d(t_d) \delta(t - t_d - t(z_b)), \quad (5)$$

where  $P_m(m_1, m_2)$  is a function of the constituent masses that encodes the mass distribution,  $R_0$  is the current merger rate, and  $Z$  is a normalization constant chosen such that

$$\mathcal{R}(z=0) = \int dm_1 dm_2 \left. \frac{d\mathcal{R}}{dm_1 dm_2} \right|_{z=0} \equiv R_0. \quad (6)$$

The redshift distribution is typically taken as the convolution of the binary formation rate  $P_b(z_b)$  with the distribution of time delays  $P_d(t_d)$  between formation and merger. Each of these distributions are specific to the population in question. For the case of the LIGO-Virgo populations (i.e., populations for which observations exist) the present-day merger rate  $R_0$  and mass distribution can be jointly determined from experimental data. In practice, this is achieved by assuming some parametric form for the mass distribution and simultaneously fitting Eq. (5) for  $R_0$  and the mass distribution parameters. In this way, one should be aware that quoted values of  $R_0$  are dependent on the mass distribution (and its parameter values) and indeed also on the assumed form of  $P_b$  and  $P_d$  which are typically taken to be fixed in the context of such fits.

Armed with this general prescription, we shall now consider a number of distinct astrophysical populations: stellar-mass BBHs, BNSs, and BHNSs. Our purpose here is twofold: first, and somewhat crucially, to highlight the relevance of astrophysical backgrounds to future long-baseline atom interferometry GW searches, and second, to demonstrate how the different elements in Eq. (3) can be modeled for known populations. In this way, the rest of this section provides essential groundwork for Sec. III in which we adapt this technology to consider the possibility of observing GW backgrounds from hypothetical populations of ECOs.

### A. Binary black holes

Thanks to the (now sizable) number of direct merger observations made by the LIGO-Virgo network [42,43,95], the distribution and merger rate of the population of  $\mathcal{O}(10M_\odot)$  BBHs are well understood [40,41]. In this way, and in contrast to the increasingly elusive and eventually hypothetical systems to which we shall later turn, calculations of the cumulative GW signal from these BBH mergers are empirically informed. Recent observations suggest that the population of stellar-mass BBHs probed by the LIGO-Virgo network have small effective spins [40]. As such, we follow Ref. [48] in assuming the BBH spins to be negligible. In proceeding, our treatment of BBHs shall largely follow the treatment and approximations of Ref. [45], which computed the (specifically stochastic) background from the stellar-mass BBH population as inferred from LIGO-Virgo observations in order to establish its implications for future measurements of subdominant cosmological backgrounds.

Provided that the BBH population probed by LIGO-Virgo is purely astrophysical, i.e., has no primordial contribution, the binary formation rate can be assumed to track the stellar formation rate (SFR), which we take to be [96]

$$\text{SFR}(z) \propto \frac{(1+z)^{2.6}}{1 + ((1+z)/3.2)^{6.2}} \equiv P_b(z). \quad (7)$$

The formation-merger delay time can be assumed to follow a simple power-law distribution  $P_d(t_d) \propto t_d^{-1}$  over  $t_{\min} < t_d < t_{\max}$  where  $t_{\min} = 50$  Myr and  $t_{\max}$  is the age of the Universe at merger  $t(z)$  [97].<sup>2</sup>

For the BBH mass distribution we adopt the parametric form introduced in Ref. [103] employed in Ref. [45] that

$$P_m(m_1, m_2) = M^\alpha \eta^\beta \psi(m_1) \psi(m_2). \quad (8)$$

Within this expression,  $M = m_1 + m_2$  is the total mass of the system and  $\eta = m_1 m_2 / (m_1 + m_2)^2$  is the symmetric mass ratio. The mass function of the constituent objects is given by  $\psi$  and is taken to be a truncated power law of the form

$$\psi(m) \propto m^\zeta \Theta(m - m_{\min}) \Theta(m_{\max} - m), \quad (9)$$

where  $\Theta$  denotes the Heaviside step function and the normalization is such that

$$\int \psi(m) d \ln m = 1. \quad (10)$$

The minimum and maximum masses within this function are taken to be  $m_{\min} = 3M_\odot$  and  $m_{\max} = 55M_\odot$ , corresponding to estimates for the maximum mass of neutron stars and the start of the pair instability mass gap, respectively<sup>3</sup> [45]. The mass dependence of astrophysical binary system formation is empirically encoded in the parameters  $\alpha$  and  $\beta$ . Following the maximum likelihood fit to the LIGO-Virgo GWTC-2 [42] event catalog of events up to and including the first half of the O3 observational run

<sup>2</sup>While we shall not consider such additional complications in this work, some studies consider more sophisticated models for BBH formation which follow the evolution of a number distinct star populations and account for differences in properties such as the optical depth to reionization and the metallicity of the interstellar medium [98–102].

<sup>3</sup>While we note that heavier mass black holes have indeed been indirectly observed at LIGO (see, e.g., Ref. [104]), we focus here on the well-characterized solar mass population. We will discuss the possibility of heavier masses, the population characteristics of which are subject to considerably greater uncertainty, in Sec. II D. The upper and lower masses used here are standard in models of the stellar-mass BBH population (see, e.g., Ref. [41]) and crucially match those adopted in Ref. [45] in which the fit from which the mass distribution parameters  $\alpha$ ,  $\beta$ , and  $\zeta$ , and the present-day merger rate  $R_0$  that we use in our calculation was performed.

performed in Ref. [103],<sup>4</sup> we adopt the values  $\alpha = 0$ ,  $\beta = 6$ ,  $\zeta = -1.5$ , and  $R_0 = 10_{-5}^{+6}$  Gpc<sup>-3</sup> yr<sup>-1</sup>.

For BBHs, the Fourier transformed signal amplitude for inspiral, merger, and ringdown phases can be respectively approximated as [105]

$$|\tilde{h}(f)| = \sqrt{\frac{5\eta}{24}} \frac{[GM(1+z)]^{5/6}}{\pi^{2/3} d_L} \times \begin{cases} f^{-7/6} & f < f_{\text{merg}} \\ f_{\text{merg}}^{-1/2} f^{-2/3} & f_{\text{merg}} \leq f < f_{\text{ring}} \\ f_{\text{merg}}^{-1/2} f_{\text{ring}}^{-2/3} \frac{\sigma^2}{4(f-f_{\text{ring}})^2 + \sigma^2} & f_{\text{ring}} \leq f < f_{\text{cut}} \\ 0 & f \geq f_{\text{cut}} \end{cases}. \quad (11)$$

The frequencies  $f_{\text{merg}}$ ,  $f_{\text{ring}}$ ,  $f_{\text{cut}}$  and the ringdown width  $\sigma$  are of the form

$$f_j = \frac{a_j \eta^2 + b_j \eta + c_j}{\pi GM(1+z)}, \quad (12)$$

with the coefficients  $a_j$ ,  $b_j$ , and  $c_j$  as listed in Ref. [105].  $d_L(z) = (1+z)/H_0 \int_0^z E(z')^{-1} dz'$  is the luminosity distance to the source and is related to the comoving distance  $d_c(z)$  by  $d_L(z) = (1+z)d_c(z)$ .

### B. Binary neutron stars

With only two recorded direct observations of mergers to date [106,107], there remains considerable uncertainty in the mass and redshift distributions of binary neutron stars and, in turn, the determination of their present-day event rate. Following the analysis in Refs. [41,48,108], we take each of the component neutron stars to follow a uniform mass distribution over the range  $1M_\odot$ – $2.5M_\odot$ . We take the BNS progenitor formation rate to be proportional to that of stellar formation as given in Eq. (7) and once again assume a time delay distribution of the form  $P_d(t_d) \propto t_d^{-1}$  for  $t_{\text{min}} < t_d < t_{\text{max}}$  where in this case  $t_{\text{min}} = 20$  Myr and  $t_{\text{max}}$  is the age of the Universe at merger  $t(z)$  [48,108]. We adopt the most up-to-date value of the present event rate given in Ref. [41] of  $R_0 = 105.5 \pm_{83.9}^{190.2}$  Gpc<sup>-3</sup> yr<sup>-1</sup>. This estimation was extracted using an alternative parametrization of the redshift distribution compared to that deployed in our

calculations, specifically in the use of a metallicity-weighted model of stellar formation rate [109]. While this choice could, in principal, have impacted the value of  $R_0$  obtained in the fit, given the magnitude of the uncertainties involved, we consider this determination sufficient for our purposes. Due to the lack of observational data, the waveforms of the postinspiral phases of BNS merger events are not well understood. As such, we follow Ref. [48] in only including contributions to  $\Omega_{\text{BNS}}$  from the inspiral phase, truncating the waveform at the frequency corresponding to the innermost stable circular orbit (ISCO) at which stage the separation of the merging objects renders a point-particle approximation invalid. For a binary system, the ISCO frequency<sup>5</sup>  $f_{\text{I}}$  (at the source) is [51]

$$f_{\text{I}} = \frac{1}{6^{3/2} \pi GM}, \quad (13)$$

where, as before,  $M$  refers to the total mass of the binary system.

### C. Black hole–neutron star binaries

The most recent LIGO-Virgo GWTC-3 event catalog [43] contains four black hole–neutron star merger events [42,110,111]. In our estimation of the GWB from these objects, we follow Ref. [41] in assuming that the neutron stars in such binary systems follow a uniform mass distribution between  $1M_\odot$  and  $2.5M_\odot$ , and that the black hole has a logarithmically uniform mass distribution between  $5M_\odot$  and  $50M_\odot$ . We take a present-day merger rate of  $R_0 = 32 \pm_{24}^{62}$  Gpc<sup>-3</sup> yr<sup>-1</sup> as determined (and deployed) in Ref. [41] and assume an identical redshift distribution to that used for BBH in Sec. II A. Since we are ultimately interested in the barrier that this background may pose to more exotic GW signatures, we wish to be conservative in our estimate of the astrophysical signal and as such include contributions to the energy from each of the inspiral, merger, and ringdown phases here, using the BBH amplitudes given in Eq. (11). We emphasize that since some proportion of BHNS inspirals are likely to terminate with tidal disruption of the neutron star [112–114], the inclusion of these contributions likely overestimates  $\Omega_{\text{BHNS}}$  at high frequencies close to merger. Given that the operational range of the experiments considered in this work will primarily be sensitive to the (lower frequency) inspiral phases of such objects, this approximation would unlikely prove problematic to our analysis.

<sup>4</sup>Although the GWTC-3 catalog [43] has been since been released, we note that the estimation of the BBH background performed in Ref. [41] using this updated catalog is not considerably changed from that which was found in Ref. [48] from the previous catalog. As such we deem the use of this mass distribution and merger rate sufficient for our purposes. A more complete discussion of the consistency of our results with the most up-to-date background estimates in Ref. [41] shall be given in Sec. II E.

<sup>5</sup>Note that this formula is the ISCO formula specifically for black holes. More rigorously one should account for object compactness  $C$ , as in Eq. (21). Here, we use the black hole compactness in order to match the approach taken by the LIGO Collaboration in Refs. [41,48]. We note that this provides a reasonable cutoff scale for this purpose and acts in the direction of balancing out the neglected contributions from postinspiral phases.

### D. Backgrounds from other astrophysical sources

Although we expect the GWB from the inspiral of stellar-mass compact binaries to largely dominate the total astrophysical background within the AION frequency band, for completeness we shall briefly comment on other potential contributions. With the absence of empirical data such as that enjoyed by the LIGO compact binaries, it is important to note that the population characteristics and potential merger rates of the astrophysical populations to be discussed here are highly uncertain and, in some cases, completely unknown, making their potential impact difficult to assess. As such, we do not include these sources in our presentation of the total astrophysical GWB in Sec. II E but shall instead limit ourselves to a predominantly qualitative discussion here. Our treatment largely follows that in Ref. [115], to which we refer the interested reader for further details.

We first turn to possible signals from intermediate-mass black holes (IMBHs), a hypothetical population of black holes with masses between  $\sim 10^2$  and  $10^4 M_\odot$  [116], of which just one indirect observation has been made [104]. While the formation mechanism of these objects is yet to be established, “runaway” mergers of massive stars in young dense stellar clusters [117] is one possibility. As such, one may postulate the existence of so-called intermediate-mass ratio inspirals (IMRIs) which arise from the mergers of stellar- and intermediate-mass black holes. The rate of such mergers would depend on a number of unknowns, not least the IMBH mass and redshift distributions. A broad-brush estimation of the background from such events is presented in Ref. [115]. Here, the IMBHs are chosen to follow a uniform mass distribution, and a merger rate is selected according to predictions of the number of IMRIs made in Ref. [116]. The resulting spectrum, which therefore also scales as  $f^{2/3}$  during inspiral, is subdominant to that of stellar-mass black holes at all frequencies. While IMBH-IMBH mergers are also possible, these events are likely to be even more rare and therefore also likely to have backgrounds inferior to their stellar-mass counterparts. We therefore do not explicitly estimate either background. Mergers between stellar-mass and supermassive black holes, so-called extreme-mass ratio inspirals (EMRIs) [116], provide another potentially sizable background. Modeling these signals is a complex process, not least because there is a large uncertainty in the merger rate and because many of the relevant population parameters are unknown. While the rough estimate of this background made in Ref. [115] places it as subdominant to the stellar-mass black hole background at the frequencies most relevant to AION, the two become comparable in a small frequency range localized around  $10^{-3}$  Hz which will be accessible to LISA and AEDGE+. Given that this estimation is subdominant to that expected from stellar-mass compact binaries at the frequencies probed

by the terrestrial long-baseline experiments and first-generation space-based atom interferometers that form the basis of this work, we do not include it in our total astrophysical background as presented in Sec. II E. Given the high uncertainty in this forecast, we note again that once more detailed data are accrued on EMRIs, a more detailed consideration of this signal is warranted in order to fully assess its relevance. The same can be said for IMRIs. In the meantime, however, one must remain mindful of these sources, particularly when attempting to interpret the origin of possible observations of “exotic” backgrounds. Finally, as argued in Ref. [115], we note that the stochastic backgrounds generated from mergers of binary supermassive black holes are typically not deemed to be relevant for midfrequency GW experiments, and neither are those from slowly rotating neutron stars or type 1a supernovae.

Although not relevant in the AION frequency band, white dwarf binaries (WDBs) become important at the lower frequencies to be reached by future space-based missions including AEDGE and LISA. The emission from these objects is weak and the background is overwhelmingly dominated by binaries from within the Galaxy. The stochastic (i.e., unresolved) Galactic WDB background spectrum, as estimated for LISA, is predicted to exceed that of stellar-mass compact binaries sub  $\sim 0.003$  Hz [118]. Being highly anisotropic, one should in principle be able to exploit the yearly modulation of this background to remove all but its isotropic component, allowing it to be neglected [119].

We thus conclude, in the absence of data on which to form more detailed models, that the other potential astrophysical backgrounds from merging binaries are either largely subdominant to that of stellar-mass binaries or excludable such that to a good approximation they can be neglected in estimations of the total astrophysical background.

### E. Analysis

In Fig. 1, we plot our estimates of the GWBs from each of the BBH, BNS, and BHNS populations individually. We display these as bands whose outer limits denote the result of adopting the upper and lower bounds of the present-day merger rate in our calculations in place of the mean value. In this way our presentation differs from that of the LIGO-Virgo Collaboration in Refs. [41,48] where the plotted bands include for the errors on the mass distribution parameters, whose values in these are determined by way of a simultaneous fit with  $R_0$  to the relevant event catalog. We observe that the contributions from the individual BBH, BNS, and BHNS share a common gradient over much of the spectrum reflective of the fact that much of the gravitational radiation is emitted during the inspiral phase, where  $\Omega \sim f^{2/3}$  independent of the nature of the binary system. In Fig. 2, we combine these distinct contributions in order to evaluate the overall implications of the total astrophysical

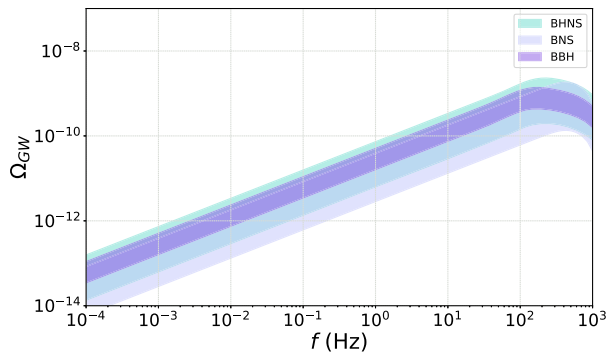


FIG. 1. Estimates of the gravitational wave backgrounds from mergers of stellar-mass BBH, BNS, and BHNS systems. The signal from BBH, BNS, and BHNS populations as inferred from observations at the LIGO-Virgo network are individually shown as bands whose upper (lower) values arise from adopting the  $1\sigma$  upper (lower) limits of the respective present-day merger rates (as given in the text) in place of their central values.

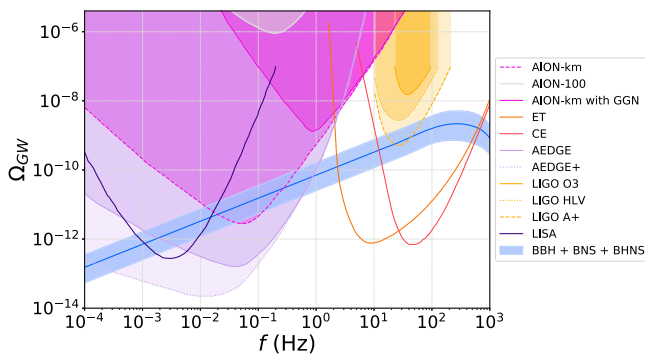


FIG. 2. An estimate of the total astrophysical GWB obtained from combining the contributions from BBH, BNS, and BHNS populations (as displayed in Fig. 1) is shown as a solid blue line. The upper (lower) limits of the blue band result from the linear addition of the upper (lower) limits of each of these populations individually. Also shown are the power-integrated (PI) [120] prospective sensitivities to power-law backgrounds of the AION-100, AION-km, AEDGE, and AEDGE+ experiments taken from Ref. [37]. We also display the predicted sensitivity of AION-km assuming that gravitational gradient noise (GGN) cannot be eliminated [37]. This estimate is based on Peterson's new low noise model (NLNM) which bounds the expected seismically induced GGN from below. The  $2\sigma$  PI curves for the recent LIGO O3 run, as well as projections for the Advanced LIGO-Virgo (HLV) network and A+ detectors operating at design sensitivities are taken from [43], and the PI prospective sensitivity of LISA [35] to power-law backgrounds is taken from Ref. [82]. Also shown are predictions for the sensitivity of the future third-generation terrestrial-based ET and CE networks. The former, taken from Ref. [121] assumes a triangle configuration of three detectors each with 10 km arm length and with both HF and LF instruments in operation. The latter, taken from Ref. [122], is for a pair of U.S.-based detectors each with 40 km arm length. Signals lying above the PI detector curves are expected to be observed with a signal-to-noise ratio  $\geq 1$  or, in the case of CE,  $\geq 3$ .

background for terrestrial long-baseline atom interferometers. The blue line shows the addition of the central estimations of the emission from BBH, BNS, and BHNS populations with the surrounding band encompassing the signals obtained from linearly adding the estimates that result from adopting the upper or lower values of the present merger rates of these two populations. In this way our estimation of the uncertainty on the total background is more conservative than that of [41,48] where a more sophisticated determination of the total signal and its related uncertainty is performed. This choice is reflective of the purpose of our work here: to assess the barrier such a background may have on searches for new, exotic fundamental physics at long-baseline atom interferometers. Since we are ultimately interested in comparing the size of the astrophysical background to hypothetical signals whose predictions suffer from considerable uncertainty and, indeed, due to our ignorance of the structure of the dark sector could lie over several orders of magnitude (see Sec. III), there is little to be gained from a precision background characterization. Of greater relevance is a conservative upper estimate of the astrophysical background which can be deployed as a handle on the magnitude of signal required from a potential beyond the Standard Model background for it to be observable. Nonetheless, we provide a brief comparison of our results with the most up-to-date LIGO-Virgo calculation performed in Ref. [41] based on the complete O3 observational run catalog GWTC-3 [43]. We find the total background (including the BBH, BNS, and BHNS contributions) to be  $\Omega_T(25 \text{ Hz}) = 6.1_{-4}^{+8} \times 10^{-10}$ , which is compatible with the value of  $\Omega_T(25 \text{ Hz}) = 6.9_{-2.1}^{+3} \times 10^{-10}$  quoted in Ref. [41]. While our prediction for  $\Omega_T$ , which is what will be actually be measured at a detector, is compatible, we do however note that our estimation of the contribution from BBHs, specifically that  $\Omega_{\text{BBH}}(25 \text{ Hz}) \sim 3_{-1.4}^{+1.6} \times 10^{-10}$ , is slightly below the value  $\Omega_{\text{BBH}}(25 \text{ Hz}) \sim 5_{-1.8}^{+1.4} \times 10^{-10}$  found in Ref. [41].<sup>6</sup> We believe this to be a result of the fact that our calculation adopts the central values of the parameters of our chosen mass distribution, whereas Ref. [41] and its precursor [48] based on the GWTC-2 catalog [42] include for the uncertainties on these values. Furthermore, we have not included a high metallicity cutoff to the SFR as in the works to which we compare. Given our arguments for the purpose of this section above, and that it is the *total* GWB from astrophysical objects that is the observable quantity (i.e., not  $\Omega_{\text{BBH}}$  individually), this difference is of little importance to our conclusions.

<sup>6</sup>A similar scenario was found in Ref. [44] which compared a prediction for  $\Omega_{\text{BBH}}$  based on the same mass distribution as the corresponding LIGO-Virgo analysis [48]. As such, we do not believe our choice of a different mass distribution (and thus present-day event rate) to Ref. [41] to have generated the discrepancy observed between these results.

To assess the detectability of an astrophysical background at future long-baseline atom interferometers, Fig. 2 also shows the PI [120] prospective sensitivities of the AION-100,<sup>7</sup> AION-km, AEDGE, and AEDGE+ experiments taken from Ref. [37]. Such curves demonstrate the (unless otherwise specified  $1\sigma$ ) sensitivity of a standard cross-correlation search [38] to power-law backgrounds, such as the  $\Omega \sim f^{2/3}$  inspiral phase of merging binary systems. PI curves are constructed from the locus of points at which power-law spectra are expected to have some specified signal-to-noise ratio (SNR), which, unless otherwise stated, should be assumed to be 1 [120]. The SNR, as defined in Ref. [38], depends on the time over which such a signal is observed, i.e., the planned experimental run time.<sup>8</sup> Such curves can be interpreted as the point above which a power-law background would be observed with a SNR exceeding the stated threshold. On this plot we also display the predicted PI sensitivity of AION-km assuming that GGN cannot be eliminated [37]. This estimation is based on Peterson’s NLNM which bounds the expected seismically induced GGN from below. Recent work in Ref. [123] is optimistic of being able to largely mitigate such effects in searches for ultralight dark matter by operating in a multi-gradiometer configuration. Further studies are needed to fully assess the potential benefits of this strategy for GW detection however. For comparison, we also display the  $2\sigma$  PI curves for the recent LIGO O3 run, in addition to projections for the HLV network and A+ detectors operating at design sensitivities [43]. The PI prospective sensitivity of LISA [35] to power-law backgrounds, taken from Ref. [82], is also shown. With timescales comparable to those of AEDGE, the PI sensitivities to power-law backgrounds of two future third-generation terrestrial gravitational wave observatories—the Einstein Telescope (ET) and Cosmic Explorer (CE)—are also considered. The displayed curve for the ET is specifically for a triangular-based configuration of three detectors each with 10 km arm length and both their high-frequency (HF) and low-frequency (LF) instruments operative [121]. For the CE, the curve, which is constructed for a threshold SNR of 3, is for a pair of U.S.-based detectors each with 40 km arm length [122]. It is clear from this plot that the total astrophysical GWB will be well within the reach of both the terrestrial AION-km experiment (assuming complete mitigation of GGN) and its space-based successors, in addition to LISA, future upgrades to LIGO, and third-generation terrestrial networks.

Although falling beyond the reach of current GW observatories (e.g., LIGO O3), the astrophysical

<sup>7</sup>This is planned as an intermediate stage between the AION-10 and AION-km experiments. Although more suited to searches for ultralight dark matter than GWs, we include it here for reference.

<sup>8</sup>This detail can be found within the referenced work for each experiment in which these curves are derived.

background is a well-motivated future target of future GW observatories which would provide complementary information to that obtained from individual merger events. By giving access to objects at higher redshifts than those in resolved detections, studies of GWBs enable the investigation of the collective properties of astrophysical populations such as their average masses, binary occurrence rate [124], and how these evolve with redshift. GWB studies have also been proposed as a means to extract information on black hole angular momentum, neutron star ellipticity [125], and neutron star magnetic fields. The opportunity to extract information pertaining to stellar formation rates and the evolution of stellar metallicities with redshift is another strong motivation which is of relevance to a number areas of astrophysics and cosmology. Theoretical studies have also looked to stochastic signals in a bid to investigate hypothetical scenarios such as multichannel astrophysical and primordial black hole mergers [126]. In addition, if the subdominant cosmological (primordial) stochastic background is to be observed in the future, as has been identified as a major scientific goal of LISA [35], this will likely demand some subtraction of the astrophysical background. By giving access to this signal in a complementary frequency range to other experiments, atom interferometers should allow for a more complete characterization and understanding of the spectral shape of the astrophysical background. In this way, they may prove crucial to the future unveiling of a cosmological stochastic background.

### III. THE ECO ZOO

Let us now consider the dark sector possibilities which could give rise to a GWB from mergers of dark compact objects. We commence with some words of motivation in Sec. III A, however, one can skip directly to Sec. III B for primarily quantitative aspects.

#### A. Motivation

The SM of particle physics is by no means minimal. At the hitherto smallest explored distance scales nature exhibits four types of gauge force, a smörgåsbord of matter fields in a variety of gauge representations with masses spanning at least 12 orders of magnitude and, inexplicably, a solitary scalar field. Given this diverse offering of microphysics it is not surprising that the SM gives rise to a cornucopia of naturally occurring phenomena over an extraordinary range of scales. At the upper end, one has composite quasistable astrophysical objects: a family of star varieties, white dwarfs, and neutron stars, all of whose stability and formation are owed to the diverse length scales embedded within those unexplained fundamental SM parameters. A universe without the massless photon, without the electron mass endowed by its interaction with the Higgs field, without the proton mass endowed by dimensional

transmutation in QCD, or without the tiny proton-neutron mass splitting endowed by the Higgs field and the quark charges, and so forth, would be very different indeed. Perhaps unimaginably so.

Given the scant information we have on the microphysics of the dark sector and the richness we observe in the visible sector it would thus seem naïve to suppose that the dark sector ought to be any less rich. We do know that the majority of the dark matter budget is not subject to strong long-range dissipative forces, but that is a very weak restriction when it comes to the potential variety of dark phenomena.

What of Occam’s razor? There are many instances in the past in which Occam’s razor, as interpreted as implying some form of “minimality” of microphenomena which counts particles, would have retrospectively failed. For instance, the atomic nucleus has, at various stages of our understanding, been a heavy charged sphere, a composite of protons and neutrons, and a composite of composites of quarks and gluons. As far as counting particles goes, it would be a flagrant violation of Occam’s razor to invoke the quarks and gluons to explain Rutherford’s scattering measurements when a simple, heavy charged point particle suffices. Yet, the quarks and gluons and their associated longer range phenomena are the truth of the matter. There is, however, reason in a view of Occam’s razor which suggests that one should work with the appropriate effective field theory at the length scales of relevance. An effective field theory contains only the degrees of freedom relevant at a given length scale. For example, an effective field theory containing only electrons and a heavy charged nucleus goes a long way if one is only interested in physics at atomic scales and longer, so why worry about the nitty gritty of QCD?

The problem with the dark sector is that we do not know at which length scale the evidence of microphysics will show up, particularly, at which “step” in the potentially rich hierarchical layers of effective descriptions of dark phenomena. If there is a similar degree of richness in the dark sector as in the visible sector then quasistable states may exist over a great range of scales and there are no guarantees as to which states will reveal themselves first. Furthermore, nongravitational interactions between the dark and visible sectors have been pursued relentlessly over great ranges of scales in an experimental program which is consistently revitalized and extended through novel detection strategies and technological developments. However, what if a rich dark sector exists, but effectively with only gravitational visible sector interactions? After all, thus far all evidence for the dark sector has been through its gravitational influence on visible matter, hence it would not be entirely surprising if this remained the case. How, then, might we reveal the richness of the dark sector?

As discussed in the Introduction, the dawn of gravitational wave astronomy has opened new eyes onto the dark

sector. We may even now hope to explore the richness of the dark sector through gravity alone. Were gravitational wave phenomena directly associated with the physics of fundamental fields detected then this would correspond to Compton wavelengths ranging from  $\sim 10^{-25}$  to  $10^{-12}$  eV. This renders macroscopic condensates of light axionlike fields in this mass range as an interesting particle physics candidate for exotic dark sector phenomena, with rich prospects (see, e.g., [127,128]), especially if such a wavelength is resonant with existing astrophysical objects such as black holes [129]. Alternatively, given a sufficiently large degree of redshifting, gravitational waves in this frequency range could be sourced by physics at much smaller distances which have, subsequent to the dynamical process, undergone cosmological redshifting. For example, early Universe phase transitions or microscopic inflationary dynamics could both have undergone significant redshifting (see, e.g., [84] for a comprehensive review).

Finally, in the SM, thanks to the universal attraction of gravity, we also have the aforementioned macroscopic objects composed of a large number of fundamental constituents held together by gravity. If such objects exist in the visible sector, then why not in the dark sector? If such ECOs [50–52] exist, then they could lead to a wide array of gravitational wave phenomena. One possibility is that one may have binary ECOs which merge giving rise to a source of gravitational waves (see, e.g., [130] for a comprehensive review). In this case, what should the characteristic frequency of such mergers be?

Given a dark sector which has its own interactions and is composed of particles at some mass scale, we should ask if there is an upper limit on the frequency of gravitational waves that could be sourced by ECOs formed of these particles? When binary orbiting ECOs are far apart, the frequency of gravitational waves may be arbitrarily low. However, as they approach one another and ultimately merge, the maximal frequency emitted will parametrically correspond to the merger frequency, which is effectively set by the radius of the objects before they touch. Thus the ECO radius is the parameter of reference. If the ECOs are more compact than their event horizon, they are necessarily a black hole, thus the minimal size limit for an ECO, and hence maximal frequency of GWs is essentially the Schwarzschild radius

$$R_{\text{Min}} = \alpha 2GM, \quad (14)$$

where  $\alpha$  is some constant satisfying  $\alpha > 1$  which is likely, at least, to be an  $\mathcal{O}(1)$  quantity. The visible sector already provides a guide where  $\alpha \gg 1$  for a white dwarf and, in practice,  $\alpha \sim \mathcal{O}(2 - 4)$  for a neutron star. Thus to determine the characteristic GW frequency it remains to determine the characteristic value of  $M$  or at least the range of masses possible.

### B. Maximal ECO masses

Consider an effective theory containing particles of mass  $m$ . These particles have gravitational interactions and, potentially, additional gauge or self-interactions characterized by a gauge coupling  $g$  or scalar self-coupling  $\lambda$ . Suppose we start with one particle at rest and add another particle. If gravity is the only interaction, or if it can overcome the mutual repulsion of other forces, then a composite object forms. Now consider continuing, adding particles *ad nauseam*. If there exists a maximum mass configuration beyond which the composite object collapses to a black hole, or some other more compact object, then what is the mass of this extremal compact object?

We may estimate this mass using dimensional analysis. We work in the same units as, for instance [131], where the dimensionless fine-structure constant is  $\alpha = e^2/4\pi\hbar c$ , with the sole exception being that we will additionally set  $c = 1$  as it offers no advantage to carry it through the equations. In these units, comparing with Newton's law of gravitation, we see that the dimensions

$$[e^2] = [G_N m^2] \quad (15)$$

match, where  $G_N$  is Newton's constant. Thus we see that the parameter combination  $G_N m^2/\hbar$  is dimensionless.

Any physical mass limit can only be expressed as a function of the fundamental parameters of the theory. These parameters include any potential couplings and the mass. Thus, if such an upper limit exists, then on dimensional grounds it will approximately take the form

$$M_{\text{Max}}^2 \approx c_{ijk} m^2 \left( \frac{\hbar}{G_N m^2} \right)^i \left( \frac{\lambda}{4\pi\hbar} \right)^j \left( \frac{g^2}{4\pi\hbar} \right)^k, \quad (16)$$

where we expect only one  $(i, j, k)$  would dominate any ultimate expression for the critical mass. The constant of proportionality is expected to be some numerical factor which is not necessarily hierarchically large or small. We expect  $i \geq 0$ , since as gravity becomes weaker the object can get more massive before gravitational collapse occurs, and  $i \neq 0$  since gravity is the only force holding the object together. Similarly, for repulsive forces we expect  $j, k \geq 0$ , as more repulsion allows for a more massive object to form without collapsing.

One obvious light example is a Planck-scale object existing independent of any supporting force  $(i, j, k) = (1, 0, 0)$ ,

$$M_{\text{Max}}^2 \propto \frac{\hbar}{G_N}. \quad (17)$$

Such an object is, however, beyond the validity of the effective theory and no definite statements can be made about it. The second possibility is  $(2, 0, 0)$ ,

$$M_{\text{Max}}^2 \propto m^2 \left( \frac{\hbar}{G_N m^2} \right)^2. \quad (18)$$

This is the smallest maximal mass one can envisage for a compact object which is supported against gravitational collapse and the factors of  $\hbar$  indicate that quantum mechanics must play a role. Indeed, this case simply corresponds to boson stars [132], whose stability against collapse is attributed to the inability to localize the field due to the uncertainty principle.

Now consider configurations which may be supported by a repulsive force which is strong enough to overcome the gravitational attraction and hence block the  $(2, 0, 0)$  case from being stable against explosion due to repulsion. Assuming a perturbative coupling, which is where we are able to trust the effective theory, the  $(2, 1, 0)$  case is lighter than the  $(2, 0, 0)$  one. Therefore, the next greatest mass is for  $(3, 1, 0)$ ,

$$M_{\text{Max}}^2 \propto \lambda \frac{\hbar^2}{G_N^3 m^4}. \quad (19)$$

Thus one could potentially have a stable object heavier than a standard boson star, supported by a repulsive force. Interestingly, this is only true if  $\lambda \gtrsim m^2/M_p^2$ , reminiscent of the weak gravity conjectures. In any case, this scenario turns out to correspond to the known self-interacting boson star scenario [133]. The gauge case scales in the same way.

Another way in which the  $(2, 0, 0)$  case could be forbidden is due to Pauli blocking. This does not involve any nongravitational interactions, thus the obvious next heaviest candidate is the  $(3, 0, 0)$  case,

$$M_{\text{Max}}^2 \propto m^2 \left( \frac{\hbar}{G_N m^2} \right)^3. \quad (20)$$

Indeed, this is none other than the Chandrasekhar limit [134] and one sees that quantum mechanics plays a significant role here.

This completes our dimensional-analysis-led study of compact object candidate maximal masses, as we have seemingly exhausted the list of potential stabilization mechanisms.

### C. A GWB from ECOs

With the various astrophysical populations that could generate a signal within the AION frequency range mapped, and the motivation for the existence of exotic compact objects explored, we now turn to estimating the GWB generated by hypothetical populations of these objects bound in binary systems. Due to our ignorance of the exact nature, specific formation details, and distributions of such objects, we will keep our analysis general, parametrizing it only in terms of the total mass  $M$  of the binary system. Given that the GWB is dominated by the inspiral phase in

which the waveform is independent of the nature of the objects involved, we will not specify ECO candidates but instead investigate the potential magnitude of signal in terms of the binary mass scale. In the absence of any empirical knowledge or theoretical motivation for the mass and redshift distributions of these objects, for simplicity we will consider all of the ECOs in a given population to have the same mass,  $M/2$ . As we did for BHNS systems, we adopt the same redshift distribution as for stellar-mass BBHs. While the waveform during the inspiral phase is known, the frequency at which this ends depends on the nature of the merging objects, as do the waveforms of the postinspiral merger and ringdown phases. It is, however, reasonable to consider the end of the inspiral phase to occur when the ISCO is reached. In general, this depends on the compactness  $C$  of the objects involved. Defining this to be the typical mass-radius ratio of the constituent objects in the binary (i.e.,  $GM/2R$  where  $R$  is the typical radius scale), the ISCO frequency as measured at the source is [51]

$$f_1^{\text{ECO}} = \frac{C^{3/2}}{3^{3/2}\pi GM}. \quad (21)$$

We note that this encompasses the black hole (BH) ISCO frequency given in Eq. (13) where the BH compactness ratio is  $1/2$ . This can be taken as an upper limit. In Fig. 3 we plot the resulting signal for various ECO masses taking the present-day merger rate to be  $R_0 = 10 \text{ Gpc}^{-3} \text{ yr}^{-1}$ , that of BBHs. Given the lack of any knowledge of merger and ringdown wave functions, we plot our estimates as bands: The lower frequency cutoff for each population is where only the inspiral signal is considered, with termination at the ISCO frequency for a value of  $C = 0.1$ , approximately that which one might expect for boson stars. The upper frequency cutoff on our bands includes contributions from inspiral, merger, and ringdown phases, employing the BH amplitudes as given in Eq. (11). This likely overestimates the high-frequency spectrum for objects of lower compactness and can therefore be considered a hard upper limit on the possible high-frequency signal.<sup>9</sup>

We see that, as the mass scale of the objects increases, the frequency at which the spectrum begins to fall off decreases. In this way, it is possible that there may exist populations of ECOs which produce large signals at AION-km and other atom interferometry experiments, but would not be seen at

<sup>9</sup>Note that the same uncertainties also afflict the interplay between resolved and unresolved background ECO contributions. Individual ECO mergers would only be resolved if their waveforms, which are likely exotic in the merger and ringdown phases, are actively searched for (see, e.g., Ref. [135]). Otherwise, signals with sufficiently large strain may be missed in dedicated searches for BH mergers. In the absence of any guide as to the likely form of these signals, searching for cumulative backgrounds thus provides a robust and general way to probe the presence of such objects across the full range of hypothetical possibilities.

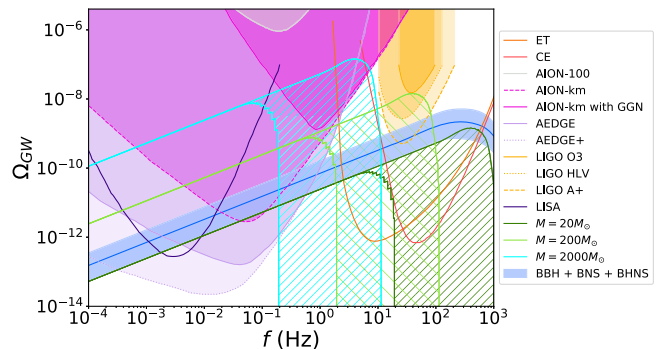


FIG. 3. An estimation of the potential signal from mergers of populations of ECOs each of mass  $M/2$  where  $M = 20, 200, 2000M_\odot$  is the total binary mass, assuming an identical redshift distribution to stellar-mass black holes and a present merger rate of  $10 \text{ Gpc}^{-3} \text{ yr}^{-1}$ . The lower frequency cutoff of each band only includes only the inspiral phase, terminating at the ISCO frequency, assuming a compactness scale of  $C = 0.1$ . The higher frequency cutoff additionally includes merger and ringdown phases, using the BH wave functions given in Eq. (11). The cumulative astrophysical GWB from BBH, BNS, and BHNS populations is shown as a solid blue line. The upper (lower) limits of the blue band result from linear additions of the upper (lower) limits of each of these populations individually. Also shown are the power-integrated [120] prospective sensitivities to power-law backgrounds of AION-100, AION-km, AEDGE, and AEDGE+ experiments taken from Ref. [37]. We also display the predicted sensitivity of AION-km assuming that GGN cannot be eliminated [37]. This estimate is based on Peterson's NLNM which bounds the expected seismically induced GGN from below. The  $2\sigma$  PI curves for the recent LIGO O3 run, as well as projections for the HLV network and A+ detectors operating at design sensitivities are taken from [43], and the PI prospective sensitivity of LISA [35] to power-law backgrounds is taken from Ref. [82]. Also shown are predictions for the sensitivity of the future third-generation terrestrial-based ET and CE networks. The former, taken from Ref. [121] assumes a triangle configuration of three detectors each with 10 km arm length and with both HF and LF instruments in operation. The latter, taken from Ref. [122], is for a pair of U.S.-based detectors each with 40 km arm length. Signals lying above the PI detector curves are expected to be observed with a signal-to-noise ratio  $\geq 1$ , or in the case of CE,  $\geq 3$ .

gravitational observatories with higher operating frequencies such as LIGO. AION thus provides us with an interesting and unique opportunity. On one hand, the observation of a GWB scaling as  $f^{2/3}$ , but with a magnitude that differs from what is expected from astrophysical objects only, would indicate the cosmological existence of ECOs. On the other hand, the possible nonobservation of this signal at the higher frequencies that are probed in complimentary GW observatories could shed light on the typical ECO mass scale and, in tandem, the properties and nature of the matter of which they are composed. However, given that backgrounds of IMRIs and EMRIs are highly uncertain, one must not be hasty in concluding that the observation of such a signal is indicative

of a population of ECOs. While we must remain open to these more “vanilla” possibilities, current estimates suggest that their backgrounds are, at most, comparable in order of magnitude to that from stellar-mass compact binaries. Any significant mismatch in amplitude between the well-characterized stellar-mass BBH background and that measured will thus warrant especially close attention, particularly if there are inconsistencies between measurements at different detectors. Until individual waveforms can actually be resolved or modeling of these astrophysical populations improves, distinguishing between these scenarios could be challenging. While the estimations considered above were made for BHs formed from the collapse of baryonic compact objects, they could in principle also form from ECOs. In this sense, the concept of observing an additional background associated with currently poorly understood classes of BH binaries is also somewhat degenerate to observing that from a population of ECOs.

While our purpose here was to consider the GWB from merging binaries of ECOs, for completeness we note that these are not the only potential sources of exotic GW emission. In particular, if ultralight bosons were to exist in nature, they may stimulate the superradiant instability of spinning black holes, resulting in the emission of near-monochromatic continuous GWs with a frequency set by the boson mass (see, e.g., Refs. [129,136,137]). Although such a signal may therefore contribute to the observed GWB, its spectral shape is predicted to considerably differ from that characteristic of inspiraling binary systems. Not only is the frequency domain covered (assuming a specific boson mass) much narrower, but the spectrum is expected to have a much steeper scaling with frequency [138–140]. Both of these features clearly distinguish any contribution to the GWB from this phenomenon from that of inspiraling binary ECOs, a diagnosis of which, we emphasize, should only be considered in the case of an anomalous signal which scales as  $\sim f^{2/3}$ .

In assessing the plausibility of observing backgrounds from ECOs it is also important to be mindful of the mass abundance of ECO binaries that would be required. Assuming that the present merger rate is  $R \text{ Gpc}^{-3} \text{ yr}^{-1}$  and that a fraction  $\epsilon$  of the total number of objects merge within a Hubble time, a population of binary systems of total mass  $M$  will harbor a fraction  $\eta$  of the total dark matter energy density  $\rho_{\text{DM}} = 0.22\rho_c$ ,

$$\eta = \frac{\rho_{\text{ECO}}}{\rho_{\text{DM}}} \approx 6.4 \times 10^{-7} \times \left(\frac{R}{10}\right) \times \left(\frac{M}{2M_{\odot}}\right) \times \left(\frac{0.01}{\epsilon}\right). \quad (22)$$

Using  $R = 10$  and taking  $\epsilon$  to be 0.01, we find that the populations plotted, which have total masses of  $M = 20, 200, 2000M_{\odot}$ , correspond to  $\eta \sim 10^{-5}, 10^{-4}$ , and  $10^{-3}$ , respectively. Hence, even if just a fraction of the dark matter budget is in binaries of ECOs, they could generate a measurable signal in terrestrial long-baseline atom

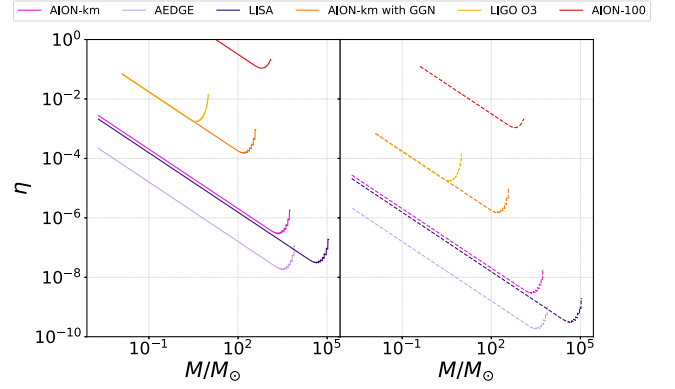


FIG. 4. A plot of the minimum fraction  $\eta$  of dark matter required to be in populations of identical mass binary ECOs as a function of total binary mass  $M$ , in order for the GWB to form a tangent to the minimum of the PI sensitivity curve of various experiments as shown in Fig. 2 (i.e., be observed with a SNR = 1). The left- and right-hand panels show the cases where the number of mergers occurring in one Hubble time correspond to 1% and 100% of the total number of binary systems, respectively, i.e.,  $\epsilon = 0.01$  and  $\epsilon = 1$ .

interferometers which could potentially be distinguishable from the expected Standard Model background. To illustrate this point further, in Fig. 4 we plot the value of  $\eta$  required for the ECO signal from different mass populations to form a tangent to the minimum of the PI sensitivity curve (i.e., be observed with a SNR of 1) of various experiments for both  $\epsilon = 0.01$  (left-hand panel) and  $\epsilon = 1$  (right-hand panel). In Fig. 5, we repeat this analysis, now plotting the minimum value of  $\eta$  required for the ECO signal to both intersect the PI sensitivity curve and exceed the total astrophysical background which, for the sake of being conservative, we take to be the upper limit on our estimate of the cumulative signal from BBH, BNS, and BHNS populations (i.e., the upper edge to the blue band in Fig. 3). Both figures corroborate the potential for discovering complexity in dark sector subcomponents.

#### D. Analytic estimates

It is useful to gain a qualitative and quantitative understanding of the results presented in Fig. 3 by performing some first-principles estimates, focusing principally on the inspiral-only curves which follow the lower frequency cutoff and are amenable to analytic estimates.

Suppose a fraction  $\eta$  of all dark matter is in the form of ECO binaries composed of equal-mass ECO binaries of total mass  $M$ . Furthermore, suppose that a fraction  $\epsilon$  of these binaries have merged between formation and now. We may derive an upper bound on the SGWB density generated by these mergers to be approximately

$$\rho_{\text{ECO}} \leq \eta \epsilon k \rho_{\text{DM}}, \quad (23)$$

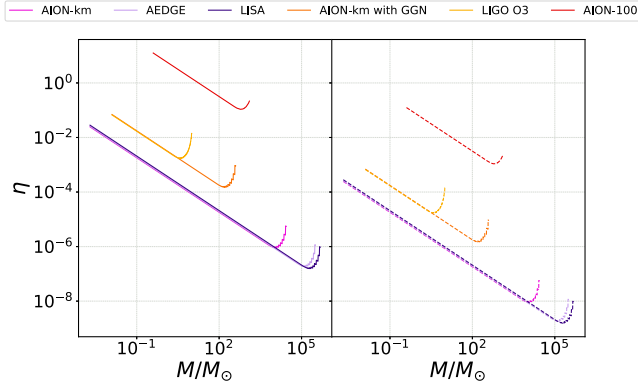


FIG. 5. A plot of the minimum fraction  $\eta$  of dark matter required to be in populations of identical mass binary ECOs as a function of total binary mass  $M$ , in order for the GWB signal to both intersect the sensitivity curve of various experiments as shown in Fig. 2 (i.e., be observed with a  $\text{SNR} \geq 1$ ) and exceed the upper limit of the total astrophysical background from BBHs, BNSs, and BHNSs (the upper edge of the blue band in Fig. 3). The left- and right-hand panels show the cases where the number of mergers occurring in one Hubble time correspond to 1% and 100% of the total number of binary systems, respectively, i.e.,  $\epsilon = 0.01$  and  $\epsilon = 1$ .

where  $\kappa$  is the fraction of rest-mass emitted in GWs for a single binary merger. Redshifting will only reduce the right-hand side, hence a bound rather than an equality. It is not possible to accurately estimate  $\kappa$  for all stages of a merger, since it depends on the details of the ECO. However, we may at least estimate the contribution to GWs up to the ISCO point. The reason is that the change in gravitational potential from the moment the binary forms to the ISCO is

$$\Delta V \approx \frac{GM^2}{4r_I}, \quad (24)$$

where  $r_I$  is the separation of the objects at the ISCO. Hence the total change in energy from the point in which the ECOs were effectively at infinite separation is

$$\Delta E \approx \frac{GM^2}{8r_I}, \quad (25)$$

where the kinetic energy change has also been included. This energy will have been radiated in GWs, thus allowing an estimate of  $\kappa$ . Taking the ISCO separation to be [51]

$$r_I \approx \frac{3GM}{2C}, \quad (26)$$

where  $C$  is the compactness ( $C = 1/2$  for a Schwarzschild black hole) and we have employed the usual Schwarzschild radius, we have

$$\kappa \approx \frac{C}{12}. \quad (27)$$

Thus, on relatively general grounds, we expect

$$\rho_{\text{ECO}} \lesssim \frac{\eta \epsilon C}{12} \rho_{\text{DM}}. \quad (28)$$

Now we recall from Sec. II that up until the ISCO the differential GW energy density emitted by a binary scales as  $f^{2/3}$ . Thus we may approximate the SGWB for an ensemble of equal-mass ECO binaries as

$$\Omega \approx \Theta(f_I - f) f^{2/3} \Omega_p, \quad (29)$$

where  $f_I$  and  $\Omega_p$  are the ISCO frequency and peak dimensionless GW energy density. Integrating this differential density over frequency up to  $f_p$  we thus find that the total GW energy density is related to the peak height as

$$\rho_{\text{ECO}} = \frac{3}{2} \Omega_p \rho_c. \quad (30)$$

Thus, putting both elements together we may estimate the GW peak height to be

$$\Omega \lesssim \frac{\eta \epsilon C \rho_{\text{DM}}}{18 \rho_c} \left( \frac{f}{f_I} \right)^{2/3}, \quad (31)$$

$$\lesssim \frac{\eta}{10^{-5}} \frac{\epsilon}{10^{-2}} \frac{C}{0.1} \left( \frac{f}{f_I} \right)^{2/3} \times 10^{-10}, \quad (32)$$

where the inspiral-only curves are cut off at  $f_I$  which was defined to be

$$f_I = \frac{C^{3/2} c^3}{3^{3/2} \pi G M}, \quad (33)$$

$$\approx \frac{400 M_\odot}{M} \left( \frac{C}{0.1} \right)^{3/2} \text{ Hz}. \quad (34)$$

Thus, with Eqs. (32) and (34) one can reliably estimate the main features of  $\Omega_{\text{GW}}$  from ECO binaries. Indeed, Eq. (32) appears to be a very good approximation to the peak heights in Fig. 3. Thus we see that the estimates provided for the inspiral phase give some physical intuition for the scale of the effect and hence some basic understanding as to why such tiny subcomponents of the dark sector could in principle generate observable signatures in future GW detectors.

#### IV. CONCLUSIONS

With the advent of gravitational wave astronomy, a new kind of light is illuminating the dark. The opportunities for advancing our knowledge of what has been hitherto hidden

from view are substantial. In this work we have concentrated on observations of a GWB at long-baseline atom interferometry experiments. In Sec. II we have focused on the signatures of known populations of celestial body binaries. Importantly, we have shown that both future terrestrial- and space-based atom interferometers could be sensitive to the GWB produced by binary populations for which the merger rate has already been estimated through observation of binary mergers by the LIGO-Virgo network [42,43,95]. As a result, atom interferometers could play a key role in plugging the frequency gap between Earth and space-based light interferometers, such as LIGO-Virgo [141] and LISA [35]. Corroborating observations of this relatively well-understood GWB between different experiments operating at different GW frequencies would essentially link our knowledge of binary populations between different stages of binary evolution. Physically, this would be through a combined measurement of the spectrum amplitude at different frequencies; this would then be compared to the logarithmic slope of the GWB, which is predicted to scale as  $f^{2/3}$  below around 100 Hz.

What if inconsistencies were found between observations at different frequencies? If such inconsistencies survived scrutiny, then they could point to new, unexpected sources of GWBs beyond the Standard Model. In Sec. III C we have shown that one potential way in which new signals could show up differently at different detectors is if there is a cosmological population of ECO binaries. Here, by “exotic” we mean that they are composed of as-yet unknown particles and by “compact” we refer to the fact that their radius would be within an order of magnitude of the Schwarzschild radius, as for neutron stars. Interestingly, such ECOs need not comprise the dominant component of the cosmological dark matter density. Rather, they could form but a tiny fraction, as for neutron stars to the

cosmological baryon matter density. While we must remain mindful of a possible degeneracy with backgrounds from currently poorly understood BH populations, the possibility of observing such a signal is certainly an exciting opportunity which could provide an important future probe of the ever-elusive dark sector.

This latter aspect reveals the importance of probing the GWB across a hierarchy of frequencies. As an example, we have shown that, due to their size, a population of ECOs whose mass satisfies  $M \gtrsim 10^3 M_\odot$  would generate a GWB which is all but invisible to the LIGO-Virgo network, but could show up with a pronounced signature at atom interferometers or LISA. This illustrates the important synergies in probing the GWB across a range of frequencies and highlights the large degree of complementarity between detection technologies.

### ACKNOWLEDGMENTS

The authors would like to thank Diego Blas, Leonardo Badurina, and John Ellis for helpful discussions on the AION project and for comments on this work. This work is supported by CERN through the Quantum Technology Initiative. Support is also provided by the U.S. Department of Energy Award No. DE-FG02-97ER-41014 (Farrell), and the U.S. Department of Energy, Office of Science, Office of Nuclear Physics, and InQubator for Quantum Simulation (IQUS) under Award No. DOE (NP) Award DE-SC0020970. This work is also supported, in part, through the Department of Physics and the College of Arts and Sciences at the University of Washington. H. B. acknowledges partial support from the STFC Consolidated HEP Grants No. ST/P000681/1 and No. ST/T000694/1 and thanks members of the Cambridge Pheno Working Group for discussions.

- 
- [1] M. S. Safronova, D. Budker, D. DeMille, D. F. J. Kimball, A. Derevianko, and C. W. Clark, Search for new physics with atoms and molecules, *Rev. Mod. Phys.* **90**, 025008 (2018).
  - [2] G. Lanfranchi, M. Pospelov, and P. Schuster, The search for feebly interacting particles, *Annu. Rev. Nucl. Part. Sci.* **71**, 279 (2021).
  - [3] P. Asenbaum, C. Overstreet, M. Kim, J. Curti, and M. A. Kasevich, Atom-Interferometric Test of the Equivalence Principle at the  $10^{-12}$  Level, *Phys. Rev. Lett.* **125**, 191101 (2020).
  - [4] L. Morel, Z. Yao, P. Cladé, and S. Guellati-Khelifa, Determination of the fine-structure constant with an accuracy of 81 parts per trillion, *Nature (London)* **588**, 61 (2020).
  - [5] G. Rosi, F. Sorrentino, L. Cacciapuoti, M. Prevedelli, and G. M. Tino, Precision measurement of the Newtonian gravitational constant using cold atoms, *Nature (London)* **510**, 518 (2014).
  - [6] J. Williams, S.-w. Chiow, N. Yu, and H. Müller, Quantum test of the equivalence principle and space-time aboard the international space station, *New J. Phys.* **18**, 025018 (2016).
  - [7] R. H. Parker, C. Yu, W. Zhong, B. Estey, and H. Müller, Measurement of the fine-structure constant as a test of the standard model, *Science* **360**, 191 (2018).
  - [8] T. Kovachy, P. Asenbaum, C. Overstreet, C. Donnelly, S. Dickerson, A. Sugarbaker, J. M. Hogan, and M. A. Kasevich, Quantum superposition at the half-metre scale, *Nature (London)* **528**, 530 (2015).

- [9] P. Hamilton, M. Jaffe, P. Haslinger, Q. Simmons, H. Müller, and J. Khoury, Atom-interferometry constraints on dark energy, *Science* **349**, 849 (2015).
- [10] R. Bouchendira, P. Cladé, S. Guellati-Khélifa, F. m. c. Nez, and F. m. c. Biraben, New Determination of the Fine Structure Constant and Test of the Quantum Electrodynamics, *Phys. Rev. Lett.* **106**, 080801 (2011).
- [11] L. Badurina *et al.*, AION: An atom interferometer observatory and network, *J. Cosmol. Astropart. Phys.* **05** (2020) 011.
- [12] M. Abe, P. Adamson, M. Borcean, D. Bortoletto, K. Bridges, S. P. Carman *et al.*, Matter-wave atomic gradiometer interferometric sensor (MAGIS-100), *Quantum Sci. Technol.* **6**, 044003 (2021).
- [13] B. Canuel, A. Bertoldi, L. Amand, E. P. di Borgo, T. Chantrait, C. Danquigny *et al.*, Exploring gravity with the MIGA large scale atom interferometer, *Sci. Rep.* **8** (2018).
- [14] J. Hartwig, S. Abend, C. Schubert, D. Schlippert, H. Ahlers, K. Posso-Trujillo, N. Gaaloul, W. Ertmer, and E. M. Rasel, Testing the universality of free fall with rubidium and ytterbium in a very large baseline atom interferometer, *New J. Phys.* **17**, 035011 (2015).
- [15] M.-S. Zhan, J. Wang, W.-T. Ni, D.-F. Gao, G. Wang, L.-X. He *et al.*, ZAIGA: Zhaoshan long-baseline atom interferometer gravitation antenna, *Int. J. Mod. Phys. D* **29**, 1940005 (2019).
- [16] G. W. Biedermann, X. Wu, L. Deslauriers, S. Roy, C. Mahadeswaraswamy, and M. A. Kasevich, Testing gravity with cold-atom interferometers, *Phys. Rev. A* **91**, 033629 (2015).
- [17] G. Rosi, G. D'Amico, L. Cacciapuoti, F. Sorrentino, M. Prevedelli, M. Zych *et al.*, Quantum test of the equivalence principle for atoms in superpositions of internal energy eigenstates, *Nat. Commun.* **8**, 5529 (2017).
- [18] S. Fray, C. A. Diez, T. W. Hänsch, and M. Weitz, Atomic Interferometer with Amplitude Gratings of Light and Its Applications to Atom Based Tests of the Equivalence Principle, *Phys. Rev. Lett.* **93**, 240404 (2004).
- [19] D. Schlippert, J. Hartwig, H. Albers, L. L. Richardson, C. Schubert, A. Roura, W. P. Schleich, W. Ertmer, and E. M. Rasel, Quantum Test of the Universality of Free Fall, *Phys. Rev. Lett.* **112**, 203002 (2014).
- [20] L. Zhou, S. Long, B. Tang, X. Chen, F. Gao, W. Peng *et al.*, Test of Equivalence Principle at  $10^{-8}$  Level by a Dual-Species Double-Diffraction Raman Atom Interferometer, *Phys. Rev. Lett.* **115**, 013004 (2015).
- [21] B. Battelier, J. Bergé, A. Bertoldi, L. Blanchet, K. Bongs, P. Bouyer *et al.*, Exploring the foundations of the physical universe with space tests of the equivalence principle, *Exp. Astron.* **51**, 1695 (2021).
- [22] P. W. Graham, D. E. Kaplan, J. Mardon, S. Rajendran, and W. A. Terrano, Dark matter direct detection with accelerometers, *Phys. Rev. D* **93**, 075029 (2016).
- [23] A. Arvanitaki, P. W. Graham, J. M. Hogan, S. Rajendran, and K. Van Tilburg, Search for light scalar dark matter with atomic gravitational wave detectors, *Phys. Rev. D* **97**, 075020 (2018).
- [24] B. Canuel, S. Abend, P. Amaro-Seoane, F. Badaracco, Q. Beauvils, A. Bertoldi *et al.*, ELGAR—a European laboratory for gravitation and atom-interferometric research, *Classical Quantum Gravity* **37**, 225017 (2020).
- [25] S. Dimopoulos, P. W. Graham, J. M. Hogan, M. A. Kasevich, and S. Rajendran, Gravitational wave detection with atom interferometry, *Phys. Lett. B* **678**, 37 (2009).
- [26] S. Dimopoulos, P. W. Graham, J. M. Hogan, M. A. Kasevich, and S. Rajendran, Atomic gravitational wave interferometric sensor, *Phys. Rev. D* **78**, 122002 (2008).
- [27] J. M. Hogan *et al.*, An atomic gravitational wave interferometric sensor in low Earth orbit (AGIS-LEO), *Gen. Relativ. Gravit.* **43**, 1953 (2011).
- [28] N. Yu and M. Tinto, Gravitational wave detection with single-laser atom interferometers, *Gen. Relativ. Gravit.* **43**, 1943 (2011).
- [29] P. W. Graham, J. M. Hogan, M. A. Kasevich, and S. Rajendran, New Method for Gravitational Wave Detection with Atomic Sensors, *Phys. Rev. Lett.* **110**, 171102 (2013).
- [30] S. Kolkowitz, I. Pikovski, N. Langellier, M. D. Lukin, R. L. Walsworth, and J. Ye, Gravitational wave detection with optical lattice atomic clocks, *Phys. Rev. D* **94**, 124043 (2016).
- [31] P. W. Graham, J. M. Hogan, M. A. Kasevich, and S. Rajendran, Resonant mode for gravitational wave detectors based on atom interferometry, *Phys. Rev. D* **94**, 104022 (2016).
- [32] P. W. Graham, J. M. Hogan, M. A. Kasevich, S. Rajendran and R. W. Romani (MAGIS Collaboration), Mid-band gravitational wave detection with precision atomic sensors, [arXiv:1711.02225](https://arxiv.org/abs/1711.02225).
- [33] B. P. Abbott, R. Abbott, T. D. Abbott, M. R. Abernathy, F. Acernese, K. Ackley *et al.* (LIGO Scientific and Virgo Collaborations), GW150914: The Advanced LIGO Detectors in the Era of First Discoveries, *Phys. Rev. Lett.* **116**, 131103 (2016).
- [34] J. R. S. and, The path to the enhanced and Advanced LIGO gravitational-wave detectors, *Classical Quantum Gravity* **26**, 114013 (2009).
- [35] P. Amaro-Seoane, H. Audley, S. Babak, J. Baker, E. Barausse, P. Bender *et al.*, Laser interferometer space antenna, [arXiv:1702.00786](https://arxiv.org/abs/1702.00786).
- [36] Y. A. El-Neaj *et al.* (AEDGE Collaboration), AEDGE: Atomic experiment for dark matter and gravity exploration in space, *Eur. Phys. J. Quantum Technol.* **7**, 6 (2020).
- [37] L. Badurina, O. Buchmueller, J. Ellis, M. Lewicki, C. McCabe, and V. Vaskonen, Prospective sensitivities of atom interferometers to gravitational waves and ultralight dark matter, *Phil. Trans. A. Math. Phys. Eng. Sci.* **380**, 20210060 (2021).
- [38] B. Allen and J. D. Romano, Detecting a stochastic background of gravitational radiation: Signal processing strategies and sensitivities, *Phys. Rev. D* **59**, 102001 (1999).
- [39] B. P. Abbott *et al.*, Sensitivity of the Advanced LIGO detectors at the beginning of gravitational wave astronomy, *Phys. Rev. D* **93**, 112004 (2016).
- [40] R. Abbott *et al.* (LIGO Scientific and Virgo Collaborations), Population properties of compact objects from the second LIGO-Virgo gravitational-wave transient catalog, *Astrophys. J. Lett.* **913**, L7 (2021).
- [41] R. Abbott, T. D. Abbott, F. Acernese, K. Ackley, C. Adams, N. Adhikari *et al.* (LIGO Scientific, Virgo, and

- KAGRA Collaborations), Population of Merging Compact Binaries Inferred Using Gravitational Waves through GWTC-3, *Phys. Rev. X* **13**, 011048 (2023).
- [42] R. Abbott *et al.* (LIGO Scientific and Virgo Collaborations), GWTC-2: Compact Binary Coalescences Observed by LIGO and Virgo during the First Half of the Third Observing Run, *Phys. Rev. X* **11**, 021053 (2021).
- [43] R. Abbott *et al.*, GWTC-3: Compact Binary Coalescences Observed by LIGO and Virgo during the Second Part of the Third Observing Run, [arXiv:2111.03606](https://arxiv.org/abs/2111.03606) [Phys. Rev. X (to be published)].
- [44] T. Regimbau, The quest for the astrophysical gravitational-wave background with terrestrial detectors, *Symmetry* **14** (2022).
- [45] M. Lewicki and V. Vaskonen, Impact of LIGO-Virgo binaries on gravitational wave background searches, *Eur. Phys. J. C* **83**, 168 (2023).
- [46] B. Abbott, R. Abbott, T. Abbott, M. Abernathy, F. Acernese, K. Ackley *et al.*, GW150914: Implications for the Stochastic Gravitational-Wave Background from Binary Black Holes, *Phys. Rev. Lett.* **116** (2016).
- [47] B. P. Abbott, R. Abbott, T. Abbott, F. Acernese, K. Ackley, C. Adams *et al.*, GW170817: Implications for the Stochastic Gravitational-Wave Background from Compact Binary Coalescences, *Phys. Rev. Lett.* **120**, 091101 (2018).
- [48] R. Abbott *et al.* (KAGRA, Virgo, and LIGO Scientific Collaborations), Upper limits on the isotropic gravitational-wave background from Advanced LIGO and Advanced Virgo's third observing run, *Phys. Rev. D* **104**, 022004 (2021).
- [49] S. Babak, C. Caprini, D. G. Figueroa, N. Karnesis, P. Marcoccia, G. Nardini *et al.*, Stochastic gravitational wave background from stellar origin binary black holes in LISA, [arXiv:2304.06368](https://arxiv.org/abs/2304.06368).
- [50] C. F. B. Macedo, P. Pani, V. Cardoso, and L. C. B. Crispino, Astrophysical signatures of boson stars: Quasinormal modes and inspiral resonances, *Phys. Rev. D* **88**, 064046 (2013).
- [51] G. F. Giudice, M. McCullough, and A. Urbano, Hunting for dark particles with gravitational waves, *J. Cosmol. Astropart. Phys.* **10** (2016) 001.
- [52] V. Cardoso, S. Hopper, C. F. B. Macedo, C. Palenzuela, and P. Pani, Gravitational-wave signatures of exotic compact objects and of quantum corrections at the horizon scale, *Phys. Rev. D* **94**, 084031 (2016).
- [53] N. Itoh, Hydrostatic equilibrium of hypothetical quark stars, *Prog. Theor. Phys.* **44**, 291 (1970).
- [54] A. R. Bodmer, Collapsed nuclei, *Phys. Rev. D* **4**, 1601 (1971).
- [55] E. Witten, Cosmic separation of phases, *Phys. Rev. D* **30**, 272 (1984).
- [56] C. Alcock, E. Farhi, and A. Olinto, Strange stars, *Astrophys. J.* **310**, 261 (1986).
- [57] J. Madsen, Physics and astrophysics of strange quark matter, *Lect. Notes Phys.* **516**, 162 (1999).
- [58] F. Weber, Strange quark matter and compact stars, *Prog. Part. Nucl. Phys.* **54**, 193 (2005).
- [59] G. Narain, J. Schaffner-Bielich, and I. N. Mishustin, Compact stars made of fermionic dark matter, *Phys. Rev. D* **74**, 063003 (2006).
- [60] L. Del Grosso, G. Franciolini, P. Pani, and A. Urbano, Fermion soliton stars, *Phys. Rev. D* **108**, 044024 (2023).
- [61] P. Jetzer, Boson stars, *Phys. Rep.* **220**, 163 (1992).
- [62] A. R. Liddle and M. S. Madsen, The structure and formation of boson stars, *Int. J. Mod. Phys. D* **01**, 101 (1992).
- [63] F. E. Schunck and E. W. Mielke, General relativistic boson stars, *Classical Quantum Gravity* **20**, R301 (2003).
- [64] S. L. Liebling and C. Palenzuela, Dynamical boson stars, *Living Rev. Relativity* **15**, 6 (2012).
- [65] L. Visinelli, Boson stars and oscillations: A review, *Int. J. Mod. Phys. D* **30**, 2130006 (2021).
- [66] E. Braaten and H. Zhang, Colloquium: The physics of axion stars, *Rev. Mod. Phys.* **91**, 041002 (2019).
- [67] C. Kouvaris and N. G. Nielsen, Asymmetric dark matter stars, *Phys. Rev. D* **92**, 063526 (2015).
- [68] R. Brito, V. Cardoso, C. A. R. Herdeiro, and E. Radu, Proca stars: Gravitating Bose–Einstein condensates of massive spin 1 particles, *Phys. Lett. B* **752**, 291 (2016).
- [69] M. I. Gresham, H. K. Lou, and K. M. Zurek, Nuclear structure of bound states of asymmetric dark matter, *Phys. Rev. D* **96**, 096012 (2017).
- [70] M. I. Gresham, H. K. Lou, and K. M. Zurek, Early Universe synthesis of asymmetric dark matter nuggets, *Phys. Rev. D* **97**, 036003 (2018).
- [71] D. M. Grabowska, T. Melia, and S. Rajendran, Detecting dark blobs, *Phys. Rev. D* **98**, 115020 (2018).
- [72] A. Coskuner, D. M. Grabowska, S. Knapen, and K. M. Zurek, Direct detection of bound states of asymmetric dark matter, *Phys. Rev. D* **100**, 035025 (2019).
- [73] Y. Bai, A. J. Long, and S. Lu, Dark quark nuggets, *Phys. Rev. D* **99**, 055047 (2019).
- [74] A. Bhoonah, J. Bramante, S. Schon, and N. Song, Detecting composite dark matter with long-range and contact interactions in gas clouds, *Phys. Rev. D* **103**, 123026 (2021).
- [75] A. Das, S. A. R. Ellis, P. C. Schuster, and K. Zhou, Stellar Shocks from Dark Matter Asteroid Impacts, *Phys. Rev. Lett.* **128**, 021101 (2022).
- [76] J. F. Acevedo, J. Bramante, and A. Goodman, Accelerating composite dark matter discovery with nuclear recoils and the Migdal effect, *Phys. Rev. D* **105**, 023012 (2022).
- [77] S. Baum, M. A. Fedderke, and P. W. Graham, Searching for dark clumps with gravitational-wave detectors, *Phys. Rev. D* **106**, 063015 (2022).
- [78] Y. Bai, J. Berger, and M. Korwar, IceCube at the frontier of macroscopic dark matter direct detection, *J. High Energy Phys.* **11** (2022) 079.
- [79] D. Croon, M. Gleiser, S. Mohapatra, and C. Sun, Gravitational radiation background from boson star binaries, *Phys. Lett. B* **783**, 158 (2018).
- [80] M. D. Diamond, D. E. Kaplan, and S. Rajendran, Binary collisions of dark matter blobs, *J. High Energy Phys.* **01** (2023) 136.
- [81] B. P. Abbott, R. Abbott, T. D. Abbott, M. R. Abernathy, F. Acernese, K. Ackley *et al.* (LIGO Scientific and Virgo Collaborations), Observation of Gravitational Waves from a Binary Black Hole Merger, *Phys. Rev. Lett.* **116**, 061102 (2016).
- [82] A. I. Renzini, B. Goncharov, A. C. Jenkins, and P. M. Meyers, Stochastic gravitational-wave backgrounds:

- Current detection efforts and future prospects, *Galaxies* **10**, 34 (2022).
- [83] P. A. Rosado, Gravitational wave background from binary systems, *Phys. Rev. D* **84**, 084004 (2011).
- [84] C. Caprini and D. G. Figueroa, Cosmological backgrounds of gravitational waves, *Classical Quantum Gravity* **35**, 163001 (2018).
- [85] K. Martinovic, P. M. Meyers, M. Sakellariadou, and N. Christensen, Simultaneous estimation of astrophysical and cosmological stochastic gravitational-wave backgrounds with terrestrial detectors, *Phys. Rev. D* **103**, 043023 (2021).
- [86] G. Boileau, N. Christensen, R. Meyer, and N. J. Cornish, Spectral separation of the stochastic gravitational-wave background for LISA: Observing both cosmological and astrophysical backgrounds, *Phys. Rev. D* **103**, 103529 (2021).
- [87] G. Boileau, A. Lamberts, N. Christensen, N. J. Cornish, and R. Meyer, Spectral separation of the stochastic gravitational-wave background for LISA: Galactic, cosmological and astrophysical backgrounds, in *55th Rencontres de Moriond on QCD and High Energy Interactions* (2021), 5, [arXiv:2105.06793](https://arxiv.org/abs/2105.06793).
- [88] M. Pieroni and E. Barausse, Foreground cleaning and template-free stochastic background extraction for LISA, *J. Cosmol. Astropart. Phys.* **07** (2020) 021.
- [89] Y. B. Ginat, V. Desjacques, R. Reischke, and H. B. Perets, Probability distribution of astrophysical gravitational-wave background fluctuations, *Phys. Rev. D* **102**, 083501 (2020).
- [90] P. A. R. Ade *et al.* (Planck Collaboration), Planck 2015 results. XIII. Cosmological parameters, *Astron. Astrophys.* **594**, A13 (2016)..
- [91] C. J. Moore, R. H. Cole, and C. P. L. Berry, Gravitational-wave sensitivity curves, *Classical Quantum Gravity* **32**, 015014 (2014).
- [92] X.-J. Zhu, E. J. Howell, D. G. Blair, and Z.-H. Zhu, On the gravitational wave background from compact binary coalescences in the band of ground-based interferometers, *Mon. Not. R. Astron. Soc.* **431**, 882 (2013).
- [93] B. S. Sathyaprakash and B. F. Schutz, Physics, astrophysics and cosmology with gravitational waves, *Living Rev. Relativity* **12**, 2 (2009).
- [94] P. C. Peters and J. Mathews, Gravitational radiation from point masses in a Keplerian orbit, *Phys. Rev.* **131**, 435 (1963).
- [95] B. P. Abbott *et al.* (LIGO Scientific and Virgo Collaborations), GWTC-1: A Gravitational-Wave Transient Catalog of Compact Binary Mergers Observed by LIGO and Virgo during the First and Second Observing Runs, *Phys. Rev. X* **9**, 031040 (2019).
- [96] P. Madau and T. Fragos, Radiation backgrounds at cosmic dawn: X-rays from compact binaries, *Astrophys. J.* **840**, 39 (2017).
- [97] K. Belczynski, D. E. Holz, T. Bulik, and R. O’Shaughnessy, The first gravitational-wave source from the isolated evolution of two stars in the 40–100 solar mass range, *Nature (London)* **534**, 512 (2016).
- [98] I. Dvorkin, E. Vangioni, J. Silk, J.-P. Uzan, and K. A. Olive, Metallicity-constrained merger rates of binary black holes and the stochastic gravitational wave background, *Mon. Not. R. Astron. Soc.* **461**, 3877 (2016).
- [99] K. Nakazato, Y. Niino, and N. Sago, Gravitational wave background from binary mergers and metallicity evolution of galaxies, *Astrophys. J.* **832**, 146 (2016).
- [100] C. Périgois, C. Belczynski, T. Bulik, and T. Regimbau, STARTRACK predictions of the stochastic gravitational-wave background from compact binary mergers, *Phys. Rev. D* **103** 043002 (2021).
- [101] G. Cusin, I. Dvorkin, C. Pitrou, and J.-P. Uzan, Properties of the stochastic astrophysical gravitational wave background: Astrophysical sources dependencies, *Phys. Rev. D* **100** 063004 (2019).
- [102] A. Mangiagli, M. Bonetti, A. Sesana, and M. Colpi, Merger rate of stellar black hole binaries above the pair-instability mass gap, *Astrophys. J.* **883**, L27 (2019).
- [103] G. Hütsi, M. Raidal, V. Vaskonen, and H. Veermäe, Two populations of LIGO-Virgo black holes, *J. Cosmol. Astropart. Phys.* **03** (2021) 068.
- [104] R. Abbott *et al.* (LIGO Scientific and Virgo Collaborations), GW190521: A Binary Black Hole Merger with a Total Mass of  $150M_{\odot}$ , *Phys. Rev. Lett.* **125**, 101102 (2020).
- [105] P. Ajith *et al.*, A Template bank for gravitational waveforms from coalescing binary black holes. I. Nonspinning binaries, *Phys. Rev. D* **77**, 104017 (2008).
- [106] B. P. Abbott *et al.* (LIGO Scientific and Virgo Collaborations), GW170817: Observation of Gravitational Waves from a Binary Neutron Star Inspiral, *Phys. Rev. Lett.* **119**, 161101 (2017).
- [107] B. P. Abbott *et al.* (LIGO Scientific and Virgo Collaborations), GW190425: Observation of a compact binary coalescence with total mass  $\sim 3.4M_{\odot}$ , *Astrophys. J. Lett.* **892**, L3 (2020).
- [108] B. P. Abbott *et al.* (LIGO Scientific and Virgo Collaborations), Search for the isotropic stochastic background using data from Advanced LIGO’s second observing run, *Phys. Rev. D* **100**, 061101 (2019).
- [109] E. Vangioni, K. A. Olive, T. Prestegard, J. Silk, P. Petitjean, and V. Mandic, The impact of star formation and gamma-ray burst rates at high redshift on cosmic chemical evolution and reionization, *Mon. Not. R. Astron. Soc.* **447**, 2575 (2015).
- [110] R. Abbott, T. D. Abbott, S. Abraham, F. Acernese, K. Ackley, A. Adams *et al.*, Observation of gravitational waves from two neutron star–black hole coalescences, *Astrophys. J. Lett.* **915**, L5 (2021).
- [111] R. Abbott *et al.*, Fermion soliton stars, [arXiv:2108.01045](https://arxiv.org/abs/2108.01045) [Phys. Rev. D (to be published)].
- [112] F. Foucart, M. D. Duez, L. E. Kidder, and S. A. Teukolsky, Black hole-neutron star mergers: Effects of the orientation of the black hole spin, *Phys. Rev. D* **83**, 024005 (2011).
- [113] K. Kawaguchi, K. Kyutoku, H. Nakano, H. Okawa, M. Shibata, and K. Taniguchi, Black hole-neutron star binary merger: Dependence on black hole spin orientation and equation of state, *Phys. Rev. D* **92**, 024014 (2015).
- [114] K. Kyutoku, M. Shibata, and K. Taniguchi, Gravitational waves from nonspinning black hole-neutron star binaries: Dependence on equations of state, *Phys. Rev. D* **82**, 044049 (2010).

- [115] B. C. Barish, S. Bird, and Y. Cui, Impact of a mid-band gravitational wave experiment on detectability of cosmological stochastic gravitational wave backgrounds, *Phys. Rev. D* **103** (2021).
- [116] P. Amaro-Seoane, J. R. Gair, M. Freitag, M. C. Miller, I. Mandel, C. J. Cutler, and S. Babak, Intermediate and extreme mass-ratio inspirals—astrophysics, science applications and detection using LISA, *Classical Quantum Gravity* **24** (2007), R113–R169.
- [117] T. Ebisuzaki, J. Makino, T. G. Tsuru, Y. Funato, S. P. Zwart, P. Hut, S. McMillan, S. Matsushita, H. Matsumoto, and R. Kawabe, Missing link found? The “runaway” path to supermassive black holes, *Astrophys. J.* **562**, L19 (2001).
- [118] T. Robson, N. J. Cornish, and C. Liu, The construction and use of LISA sensitivity curves, *Classical Quantum Gravity* **36**, 105011 (2019).
- [119] M. Pieroni and E. Barausse, Foreground cleaning and template-free stochastic background extraction for LISA, *J. Cosmol. Astropart. Phys.* **07** (2020) 021.
- [120] E. Thrane and J. D. Romano, Sensitivity curves for searches for gravitational-wave backgrounds, *Phys. Rev. D* **88**, 124032 (2013).
- [121] M. Branchesi *et al.*, Science with the Einstein Telescope: a comparison of different designs, [arXiv:2303.15923](https://arxiv.org/abs/2303.15923).
- [122] M. Evans *et al.*, A horizon study for cosmic explorer: Science, observatories, and community, [arXiv:2109.09882](https://arxiv.org/abs/2109.09882).
- [123] L. Badurina, V. Gibson, C. McCabe, and J. Mitchell, Ultralight dark matter searches at the sub-Hz frontier with atom multi-gradiometry, *Phys. Rev. D* **107**, 055002 (2023).
- [124] T. Regimbau, The astrophysical gravitational wave stochastic background, *Res. Astron. Astrophys.* **11**, 369 (2011).
- [125] F. D. Lillo, J. Suresh, and A. L. Miller, Stochastic gravitational-wave background searches and constraints on neutron-star ellipticity, *Mon. Not. R. Astron. Soc.* **513**, 1105 (2022).
- [126] S. S. Bavera, G. Franciolini, G. Cusin, A. Riotto, M. Zevin, and T. Fragos, Stochastic gravitational-wave background as a tool for investigating multi-channel astrophysical and primordial black-hole mergers, *Astron. Astrophys.* **660**, A26 (2022).
- [127] A. Arvanitaki, S. Dimopoulos, S. Dubovsky, N. Kaloper, and J. March-Russell, String axiverse, *Phys. Rev. D* **81**, 123530 (2010).
- [128] A. Arvanitaki, M. Baryakhtar, S. Dimopoulos, S. Dubovsky, and R. Lasenby, Black hole mergers and the QCD axion at Advanced LIGO, *Phys. Rev. D* **95**, 043001 (2017).
- [129] A. Arvanitaki, M. Baryakhtar, and X. Huang, Discovering the QCD axion with black holes and gravitational waves, *Phys. Rev. D* **91**, 084011 (2015).
- [130] V. Cardoso and P. Pani, Testing the nature of dark compact objects: A status report, *Living Rev. Relativity* **22**, 4 (2019).
- [131] J. S. Schwinger, Quantum electrodynamics. I A covariant formulation, *Phys. Rev.* **74**, 1439 (1948).
- [132] D. J. Kaup, Klein-Gordon Geon, *Phys. Rev.* **172**, 1331 (1968).
- [133] M. Colpi, S. L. Shapiro, and I. Wasserman, Boson Stars: Gravitational Equilibria of Self-Interacting Scalar Fields, *Phys. Rev. Lett.* **57**, 2485 (1986).
- [134] S. Chandrasekhar and E. A. Milne, The highly collapsed configurations of a stellar mass, *Mon. Not. R. Astron. Soc.* **91**, 456 (1931).
- [135] J. C. Bustillo, N. Sanchis-Gual, A. Torres-Forné, J. A. Font, A. Vajpeyi, R. Smith, C. Herdeiro, E. Radu, and S. H. W. Leong, GW190521 as a Merger of Proca Stars: A Potential New Vector Boson of  $8.7 \times 10^{-13}$  eV, *Phys. Rev. Lett.* **126**, 081101 (2021).
- [136] A. Arvanitaki and S. Dubovsky, Exploring the string axiverse with precision black hole physics, *Phys. Rev. D* **83**, 044026 (2011).
- [137] C. Palomba *et al.*, Direct Constraints on Ultra-Light Boson Mass from Searches for Continuous Gravitational Waves, *Phys. Rev. Lett.* **123**, 171101 (2019).
- [138] R. Brito, S. Ghosh, E. Barausse, E. Berti, V. Cardoso, I. Dvorkin, A. Klein, and P. Pani, Gravitational wave searches for ultralight bosons with LIGO and LISA, *Phys. Rev. D* **96**, 064050 (2017).
- [139] R. Brito, S. Ghosh, E. Barausse, E. Berti, V. Cardoso, I. Dvorkin, A. Klein, and P. Pani, Stochastic and Resolvable Gravitational Waves from Ultralight Bosons, *Phys. Rev. Lett.* **119**, 131101 (2017).
- [140] L. Tsukada, R. Brito, W. E. East, and N. Siemonsen, Modeling and searching for a stochastic gravitational-wave background from ultralight vector bosons, *Phys. Rev. D* **103**, 083005 (2021).
- [141] B. P. Abbott, R. Abbott, R. Adhikari, P. Ajith, B. Allen, G. Allen *et al.*, LIGO: The laser interferometer gravitational-wave observatory, *Rep. Prog. Phys.* **72**, 076901 (2009).